Novel Small-Molecule PGC-1α Transcriptional Regulator With Beneficial Effects on Diabetic *db/db* Mice

Li-Na Zhang, Hua-Yong Zhou, Yan-Yun Fu, Yuan-Yuan Li, Fang Wu, Min Gu, Ling-Yan Wu, Chun-Mei Xia, Tian-Cheng Dong, Jing-Ya Li, Jing-Kang Shen, and Jia Li

Peroxisome proliferator–activated receptor-γ coactivator-1α (PGC-1α) has been shown to influence energy metabolism. Hence, we explored a strategy to target *PGC-1α* expression to treat metabolic syndromes. We developed a high-throughput screening assay that uses the human *PGC-1α* promoter to drive expression of luciferase. The effects of lead compound stimulation on *PGC-1α* expression in muscle cells and hepatocytes were investigated in vitro and in vivo. A novel small molecule, ZLN005, led to changes in PGC-1α mRNA levels, glucose uptake, and fatty acid oxidation in L6 myotubes. Activation of AMP-activated protein kinase was involved in the induction of *PGC-1α* expression. In diabetic *db/db* mice, chronic administration of ZLN005 increased *PGC-1α* and downstream gene transcription in skeletal muscle, whereas hepatic *PGC-1α* and gluconeogenesis genes were reduced. ZLN005 increased fat oxidation and improved the glucose tolerance, pyruvate tolerance, and insulin sensitivity of diabetic *db/db* mice. Hyperglycemia and dyslipidemia also were ameliorated after treatment with ZLN005. Our results demonstrated that a novel small molecule selectively elevated the expression of *PGC-1α* in myotubes and skeletal muscle and exerted promising therapeutic effects for treating type 2 diabetes.
***Diabetes* 62:1297–1307, 2013**

Peroxisome proliferator–activated receptor-γ coactivator-1α (PGC-1α) serves as an inducible coregulator in the control of energy homeostasis (1–4). It is expressed abundantly in tissues with high energy demand, including brown adipose tissue, heart, skeletal muscle, kidney, and brain (5–7). It has been shown to regulate adaptive thermogenesis, mitochondrial biogenesis, glucose and fatty acid metabolism, the peripheral circadian clock, fiber-type switching in skeletal muscle, and heart development (8–11).

Dysregulation of PGC-1α was reported to be correlated with the development of insulin resistance and type 2 diabetes mellitus (T2DM) (12). Studies have reported polymorphism in the coding region of the *PGC-1α* gene, and specific promoter haplotypes are associated with an increased risk of T2DM (13–18). Hepatic expression of *PGC-1α* and its cotranscription activity are increased significantly in multiple rodent models of diabetes and obesity, including mice that received a high-fat diet, were leptin deficient (*ob/ob*) and were administered streptozotocin (19). With adenoviral delivery of PGC-1α RNA interference to the liver, mice experienced fasting hypoglycemia and enhanced hepatic insulin sensitivity (20).

Meanwhile, gene expression profiling indicated that expression of *PGC-1α* was diminished in the skeletal muscle of prediabetic humans and those with T2DM, and the expression of nuclear respiratory factor (*NRF*)–dependent genes involved in metabolic pathways and mitochondrial components was also reduced, which may have contributed to the metabolic disturbances characteristic of insulin resistance and T2DM (21–23). Evidence from skeletal muscle suggested that PGC-1α might be protective for the development of insulin resistance. Ectopic expression of *PGC-1α* in muscle cells recovered expression of insulin-sensitive *GLUT4* by coordinating the transcriptional myocyte enhancer factor 2 (MEF2)C on the promoter (24). Increased muscle expression of *PGC-1α* showed improvement in metabolic responses, as evidenced by increased insulin sensitivity and insulin signaling in aged mice (25). These results suggest that PGC-1α, a critical booster of mitochondrial function, is an excellent candidate for preventing insulin resistance and metabolic syndromes secondary to mitochondrial dysfunction (21–23). The results also highlight the importance of targeting the PGC-1α modulator to specific tissues and its efficacy in metabolic disease models.

We describe here a high-throughput screening (HTS) assay for the discovery of transcriptional modulators based on *PGC-1α* promoters. The lead compound was identified with selective stimulation of expression of *PGC-1α* in myotubes and proved to have beneficial effects on *db/db* mice.

RESEARCH DESIGN AND METHODS

Materials. Forskolin, luciferase, and luciferase antibody were obtained from Sigma-Aldrich. The 2600-base pair *PGC-1α* promoter, delta MEF and delta CRE binding element promoter-driven luciferase reporter plasmids, were obtained from Addgene. Radiolabeled [9,10-^{3}H(N)]-palmitic acid was purchased from PerkinElmer. The transfection reagent Lipofectamine 2000 was obtained from Invitrogen, and the siLentFect lipid was obtained from Bio-Rad. Luciferase substrate was purchased from Promega. Antibodies against cAMP response element- binding protein (CREBP), phospho-CREBP (Ser133), p38 mitogen-activated protein kinase (MAPK), and phospho-p38 MAPK (Thr180/Tyr182) were purchased from Cell Signaling Technology; the antibody against muscle actin was from Santa Cruz. Other materials were obtained as previously described (26).

Establishment of stable cell lines. A pGL3-basic luciferase reporter plasmid containing the 2600-base pair *PGC-1α* promoter (27) and pcDNA3.1, in a ratio of 10:1 (0.8 μg of total DNA per well), were cotransfected into HEK293 cells in a 24-well plate by Lipofectamine 2000. Stable cell lines (PGC-1α-luc) were selected based on their resistance to 1 mg/mL G418 and a strong luciferase enzyme signal.

HTS assay. Stable HEK293 PGC-1α-luc cells were plated into 384-well plates at approximately 3000 cells per well. After overnight culture, compounds at a final concentration of 2 μg/mL were added to the culture medium. At the end

From the State Key Laboratory of Drug Research, Shanghai Institute of Materia Medica, Chinese Academy of Sciences, Shanghai, China.
Corresponding authors: Jia Li, jli@mail.shcnc.ac.cn, Jing-Ya Li, jyli@mail.shcnc.ac.cn, or Jing-Kang Shen, jkshen@mail.shcnc.ac.cn.
Received 2 June 2012 and accepted 17 October 2012.
DOI: 10.2337/db12-0703
This article contains Supplementary Data online at http://diabetes.diabetesjournals.org/lookup/suppl/doi:10.2337/db12-0703/-/DC1.

of 24 h, luciferase substrate was added to each well and the released luciferin signal then was detected using an EnVision microplate reader.

Luciferase enzyme assay. Luciferase was diluted to 20 units and incubated with compounds in a 384-well plate. Then, luciferase substrate was added, and the released luciferin signal was detected using an EnVision microplate reader.

Measurement of fatty acid oxidation. The assay was initiated by adding [9,10–^{3}H(N)]-palmitic acid to a final concentration of 250 μmol/L and 1.5 μCi per well in Dulbecco's modified Eagle's medium (DMEM). After incubation with the compound for 4 h in differentiated L6 myotubes, a sample from each well was added to charcoal slurry for centrifugation and then the radioactivity was measured.

Transfection. For plasmid transfection, L6 myoblasts were transfected with Lipofectamine 2000 containing the pGL-3 basic vector, *PGC-1α* promoter luciferase, delta MEF, or delta CRE promoter luciferase. Six hours after transfection, the medium was changed for differentiation. After being cultured overnight, the cells were incubated with compound for 24 h. For transfection of small interfering RNA (siRNA), 20 nmol/L siRNA (sense: GAUUCAAACUCAGACGAUU; antisense: AAUCGUCUGAGUUUGAAUC) targeting *PGC-1α* was transfected on day 4 of L6 myotube differentiation using siLentFect lipid in serum-free DMEM. Six hours after transfection, the medium was replaced with normal medium. The next day, the cells were treated with compound for 24 h for studies.

Animal experiments. The animal experiments were approved by the Animal Ethics Committee of the Shanghai Institute of Materia Medica. Male C57BKS *db/db* and lean littermate C57BKS mice were housed in a temperature-controlled room (22 ± 2°C) with a 12-h light/dark cycle. For the pharmacokinetic studies, a single dose of ZLN005 was administered to *db/db* mice. The plasma and tissue samples were collected at different time points, and the compound concentrations were determined by liquid chromatography–mass spectrometry/mass spectrometry. For chronic treatment, six to eight 8-week-old mice were assigned randomly to the various treatment groups by body weight and glucose levels. Lean and *db/db* mice received oral administration of either vehicle (0.5% methylcellulose), ZLN005, or metformin for 6 weeks. Body weight and food intake were recorded daily. Fasting blood glucose levels were measured after 6 h of fasting. At the 3rd week of treatment, the effect of chronic ZLN005 administration on the respiratory exchange ratio (RER) of *db/db* mice was measured using an eight-chamber indirect calorimeter. The glucose tolerance test (1.5 g · kg^{-1} glucose i.p.) and insulin tolerance test (1 unit · kg^{-1} insulin i.p.) were performed after 6 h of starvation. The pyruvate tolerance test (PTT; 1.5 g · kg^{-1} sodium pyruvate i.p.) was performed in mice that had been fasted overnight. Plasma concentrations of nonesterified fatty acids (NEFAs), triglycerides, and insulin were measured as previously described (26). Plasma β-hydroxybutyrate was measured using a β-hydroxybutyrate assay kit (Abcam). At the end of treatment, the animals were killed, and their tissues were freeze-clamped for further experiments. For preliminary safety evaluation, Sprague-Dawley rats were orally administered either vehicle or ZLN005 for 14 days. The rats were checked every day for death and clinical symptoms. At day 15, the animals were anatomized and blood was collected for further investigation.

Mitochondrial DNA quantification, adenine nucleotide measurement, mitochondria respiration, and sulforhodamine B. These assays were performed as previously described (26,28–31).

Cell culture, Western blot, glucose uptake, glucose production, and real-time PCR. These assays were performed as previously described (26). In addition, HEK293 cells were cultured in high-glucose DMEM supplemented with 10% FBS. For real-time PCR, all samples were run in duplex and normalized to actin or tubulin expression. For details of primer sequences, see Supplementary Table 1.

Statistical analysis. The results are presented as the mean ± SE. Differences between the groups were analyzed with the Student's *t* test. $P < 0.05$ was regarded as statistically significant.

RESULTS

ZLN005 increases expression of the *PGC-1α* gene in L6 myotubes. Studies have shown an inverse correlation between levels of PCG-1α in muscle and mitochondrial activity, insulin resistance, and T2DM (32,33). Therefore, we created an HEK293 stable cell line containing luciferase expression driven by the human *PGC-1α* promoter (PGC-1α-luc); then the luciferase reporter assay was optimized for application in automated HTS. After we randomly screened a library containing 48,000 pure synthetic compounds with diverse structures, the novel compound ZLN027 (Supplementary Fig. 1*A*) was found to increase the *PGC-1α* promoter reporter by l.7-fold (Supplementary Fig. 1*B*). Forskolin and dexamethasone, which were reported to stimulate expression of *PGC-1α*, had stimulatory effects at 1.4- and 2.0-fold, respectively. By checking the cell survival rate, we found obvious cytotoxicity for ZLN027 in HEK293 and L6 myotubes. Extensive data mining identified another compound, ZLN005 (Fig. 1*A*), which had the same chemical backbone but did not have obvious cytotoxicity (Supplementary Fig. 1*D* and *E*). ZLN005 was observed to potently inhibit luciferases, but ZLN027 was not (Supplementary Fig. 1*C*). These results might explain the discrepancy between the two compounds in the *PGC-1α* promoter reporter assay. The transcriptional modulatory effect of ZLN005 in L6 myotubes was also investigated. As shown in Fig. 1*B*, ZLN005 increased *PGC-1α* mRNA levels in a dose-dependent manner; 20 μmol/L ZLN005 caused a threefold increase over the control after 24 h. At 10 μmol/L, the *PGC-1α* mRNA levels were increased to almost the same extent at 16 to 48 h (Fig. 1*C*).

PGC-1α is a powerful transcriptional coregulator of *GLUT4* and mitochondrial genes, including components of the electron transport system. As seen in Fig. 1*D*, the mRNA levels of *GLUT4*, *NRF1*, estrogen-related receptor α (*ERRα*), cytochrome c oxidase 5b (*cox5b*), and acyl-CoA oxidase (24,34) were increased by ZLN005 (10 μmol/L).

Because GLUT4 plays a crucial role in glucose uptake in skeletal muscle, we investigated this effect of ZLN005 further. As shown in Fig. 1*E*, ZLN005 stimulated glucose uptake dose dependently after 24 h of treatment, with 20 μmol/L of ZLN005 resulting in a 1.8-fold improvement. Because the induction of the expression of genes involved in mitochondrial biogenesis and fatty acid oxidation (FAO) (35) was observed. As shown in Fig. 1*F*, ZLN005 increased oxidation of palmitic acid dose dependently, with 20 μmol/L ZLN005 resulting in a 1.28-fold increase after 24 h compared with control. These results demonstrated that ZLN005 stimulated the expression of *PGC-1α* and downstream genes in skeletal muscle cells and improved glucose utilization and FAO.

ZLN005 did not increase the expression of the *PGC-1α* gene in rat primary hepatocytes. Gluconeogenesis plays an important role in regulating glucose levels, and PGC-1α is known to stimulate this process (36). ZLN005 had no effect on levels of *PGC-1α* mRNA in rat primary hepatocytes after 24 h of treatment (Fig. 2*A*). The expression of the key gluconeogenic enzyme coregulated by PGC-1α, phosphoenolpyruvate carboxykinase (*PEPCK*), was not affected by ZLN005 (Fig. 2*B*), nor did ZLN005 increase glucose production (Fig. 2*C*) in primary hepatocytes. The contrary effects of ZLN005 in L6 myotubes and primary hepatocytes suggested that expression of *PGC-1α* was regulated in a cell type–specific manner.

AMP-activated protein kinase is involved in the mechanism inducing *PGC-1α* in L6 myotubes. To evaluate the dependence of PGC-1α in the effects of ZLN005, L6 myotubes were transfected with *PGC-1α* siRNA. ZLN005-stimulated expression of the *PGC-1α* gene and oxidation of palmitic acid was blocked upon *PGC-1α* silencing (Fig. 3*A* and *B*). This indicated that ZLN005-stimulated FAO was mediated by PGC-1α.

To clarify the mechanism of ZLN005 acting on *PGC-1α*, transfection of the *PGC-1α* promoter harboring truncated mutations in the MEF2 and CREBP binding sites were analyzed (27). Because ZLN005 inhibits luciferase activity, luciferase protein levels were investigated as the direct

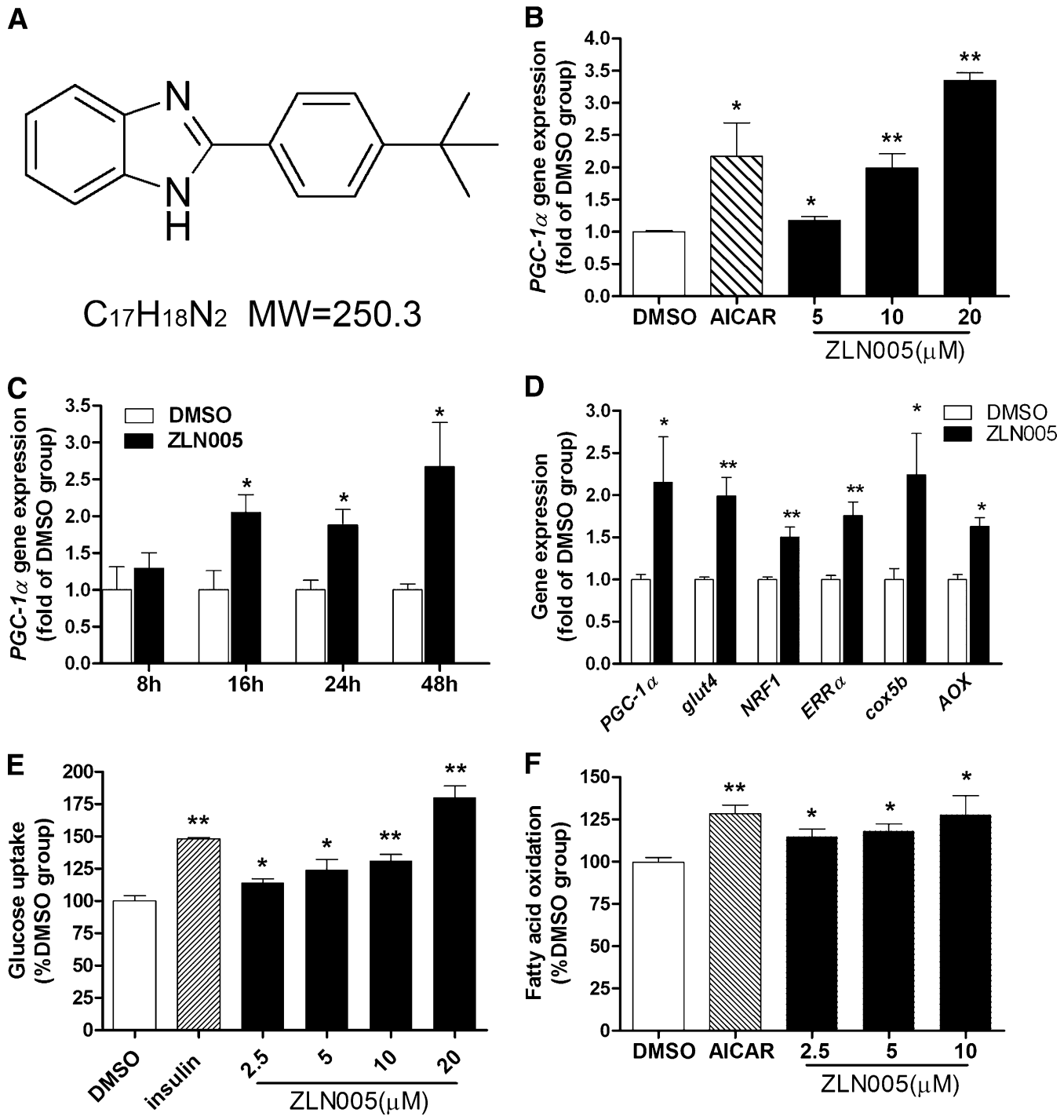

FIG. 1. ZLN005 increases expression of the *PGC-1α* gene in L6 myotubes. L6 myotubes were differentiated for 4–6 days. *A*: The structure of ZLN005 (molecular weight 250.3). *B*: Dose-dependent effect of ZLN005 on *PGC-1α* mRNA levels. L6 myotubes were treated for 24 h with different doses of ZLN005 or 1 mmol/L AICAR as a positive control. *C*: Time course of ZLN005 on *PGC-1α* mRNA levels. *D*: Effect of ZLN005 (10 μmol/L) on relative mRNA levels. *E*: Dose-dependent effect of ZLN005 on glucose uptake over 24 h. Insulin (100 nmol/L) was added in the last 30 min. *F*: Dose-dependent effect of ZLN005 on palmitic acid oxidation over 24 h. Radioactive medium containing compounds of interest was changed at the start of the last 4 h. Two millimolar AICAR was also added in the last 4 h. *$P < 0.05$, **$P < 0.01$ compared with DMSO.

readout for transcriptional activity. The *PGC-1α* promoter drives luciferase induction upon treatment with ZLN005 (10 μmol/L), but the promoter constructs with the truncated CREBP binding site showed little difference compared with the *PGC-1α* promoter. However, a truncated MEF2 binding site resulted in an ablation of the increase in luciferase protein in response to treatment with ZLN005 (Fig. 3*C*). This suggested that ZLN005 stimulation of *PGC-1α* expression was dependent on the MEF2 binding site.

Studies have reported that p38 MAPK, the energy sensor protein AMP-activated protein kinase (AMPK), and cAMP-responsive CREBP signaling pathways control expression of PGC-1α (37,38). Therefore, we determined whether treatment of L6 myotubes with ZLN005 (10 μmol/L) would lead to activation of AMPK, p38 MAPK, or CREBP. Phosphorylation levels of p38, which phosphorylates and activates MEF2 (39) and phosphorylates PGC-1α protein (40), slightly decreased, suggesting the p38 pathway was not the

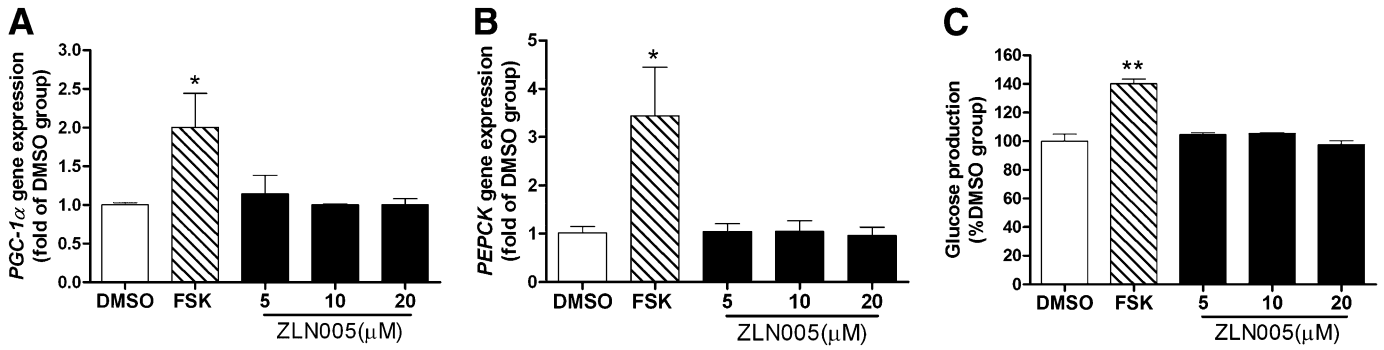

FIG. 2. ZLN005 has no effect on the expression of the *PGC-1α* gene in rat primary hepatocytes. *A* and *B*: Effects of ZLN005 on *PGC-1α* and *PEPCK* mRNA levels. Rat primary hepatocytes were treated for 24 h with different doses of ZLN005 using forskolin (10 μmol/L) as a positive control. *C*: Effect on glucose output in primary hepatocytes after 20 h of treatment. The glucose production medium was changed 4 h from the end of incubation. *$P < 0.05$, **$P < 0.01$ compared with DMSO.

cause of the increased expression of *PGC-1α*. Phosphorylation of CREBP remained unchanged, which was consistent with the previously observed lack of effect on luciferase expression for the CREBP binding site. Meanwhile, the phosphorylation of AMPK and its downstream acetyl-CoA carboxylase (ACC) were increased significantly (Fig. 3*D*).

The dose-dependent activation of AMPK by ZLN005 was confirmed at 24 h (Fig. 3*E*). Thus we examined whether the effects of ZLN005 on glucose uptake were dependent

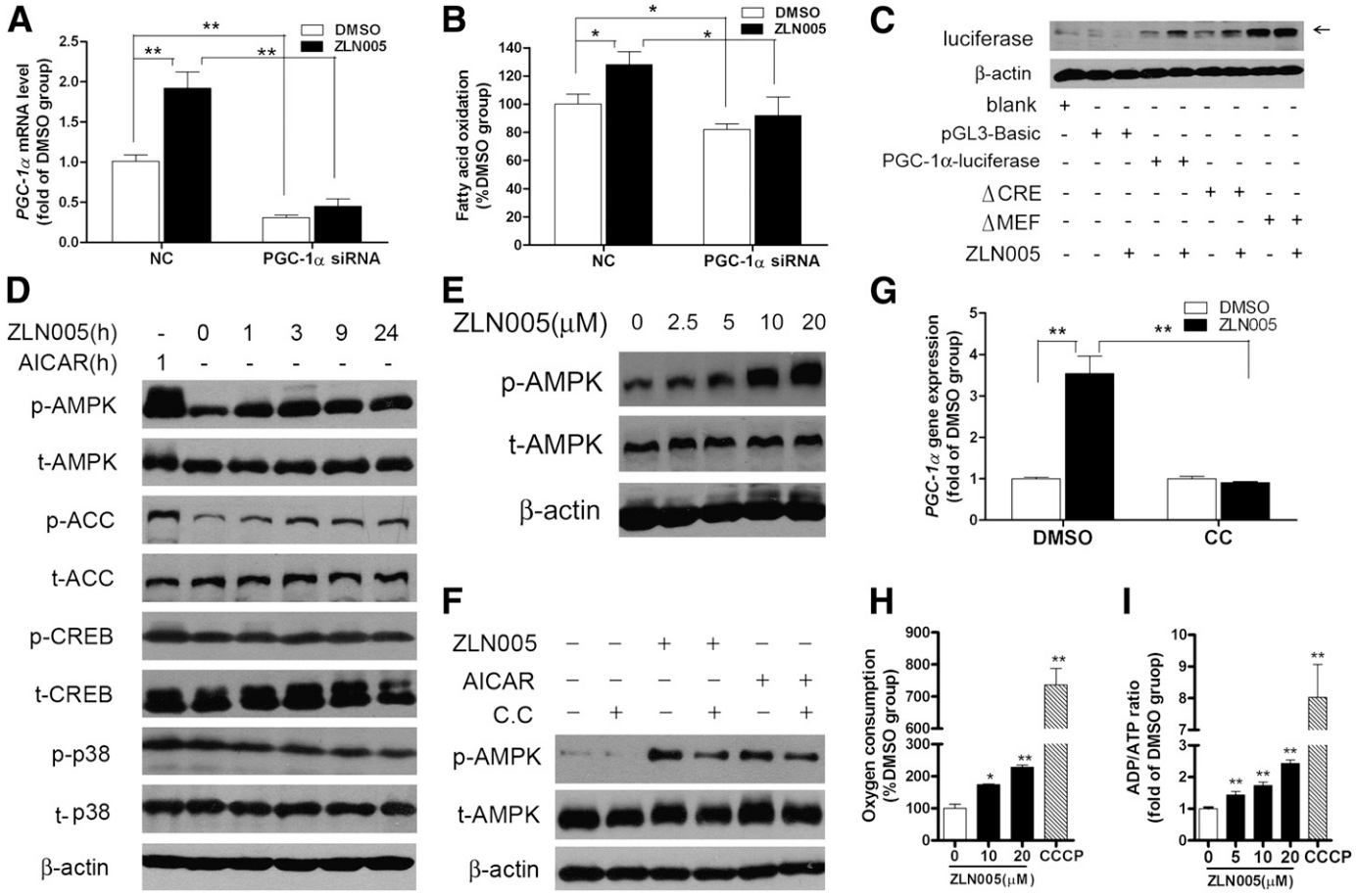

FIG. 3. AMPK is involved in the mechanism of PGC-1α induction in L6 myotubes. *A* and *B*: Effects of ZLN005 (10 μmol/L) in L6 myotubes on *PGC-1α* expression and palmitic acid oxidation after PGC-1α silencing. The controls were transfected with a scramble RNA (NC). *C*: The wild-type *PGC-1α* promoter with luciferase reporter or containing mutations in the MEF or CRE sites were transfected into L6 myoblasts and treated with 10 μmol/L ZLN005 after differentiation. Luciferase protein levels were detected by Western blot. The blank represents untransfected L6 that differentiated for the same time period. *D*: Effects of ZLN005 (10 μmol/L) on p38 mitogen-activated protein kinase, AMPK, and CREB phosphorylation in L6 myotubes at different times by Western blot. AICAR (1 mmol/L) was used as a positive control. *E*: Effect of ZLN005 on AMPK phosphorylation in L6 myotubes at 24 h by Western blots. *F*: Influence of compound C (CC) on ZLN005-induced AMPK activation. CC (5 μmol/L) was added 30 min before and during incubation with ZLN005 (20 μmol/L), DMSO, or AICAR (1 mmol/L) for 24 h. *G*: Influence of CC (5 μmol/L) on ZLN005-induced (20 μmol/L) increase in *PGC-1α* mRNA levels over 24 h. *H*: Influence of CCCP (10 μM) and ZLN005 on ADP/ATP ratio for 3 h. *I*: Effect of CCCP (4 μM) and ZLN005 on muscle mitochondria respiration. *$P < 0.05$, **$P < 0.01$ compared with DMSO.

on AMPK using the AMPK inhibitor compound C. Pretreatment with compound C attenuated the ability of ZLN005 to induce phosphorylation of AMPK and expression of *PGC-1α* (Fig. 3*F* and *G*). These results suggested that *PGC-1α* expression stimulated by ZLN005 in L6 myotubes was dependent on the AMPK pathway. To investigate the mechanism of AMPK activation by ZLN005, we measured the direct effect of ZLN005 on AMPKα2β1γ1 and AMPKα2β2γ1 on a molecular level, and no catalytic kinase activation was observed (data not shown). We found it could increase the ADP-to-ATP ratio in L6 myotubes (Fig. 3*H*) and mildly increase oxygen consumption in isolated muscle mitochondria (Fig. 3*I*). This suggests that ZLN005 increases the ADP-to-ATP ratio to activate AMPK by uncoupling mitochondria respiration in L6 myotubes.

Chronic effects of ZLN005 on the RER. Pharmacokinetic studies of *db/db* mice showed that ZLN005 was absorbed into the plasma quickly, reaching a concentration of 3.7 μmol/L within 15 min. The concentration declined to 0.44 μmol/L within 4 h (Fig. 4*A*) after a single oral dose of 15 mg/kg. ZLN005 reached a fairly high concentration of 60.9 μmol/L within 15 min in liver tissue, which then declined to 10.9 μmol/L within 4 h (Fig. 4*B*).The concentration of ZLN005 in muscle tissue was stable at approximately 3–4 μmol/L over 4 h.

Because PGC-1α is a key regulator of oxidative metabolism, we studied the effects of ZLN005 on whole-body fat oxidation using indirect calorimetry. The *db/db* mice were dosed with ZLN005 (15 mg · kg^{-1} · day^{-1}) or vehicle for 2 weeks. The last administration was given 4 h before the experiment. The animals were monitored for oxygen consumption and CO_2 production for 21 h (between 1700 and 1400 h). There were no significant changes in V_{O_2} and V_{CO_2} (Fig. 4*C* and *D*), but a decrease in the RER was observed, indicating a shift to fatty acid use (Fig. 4*E*). The heat was almost unchanged during the 21-h measurement, except for a slight increase during cycles 11 to 20 (Fig. 4*F*).

Chronic antidiabetic efficacy of ZLN005. To assess the antidiabetic efficacy of ZLN005 in vivo, we investigated the effect of chronic ZLN005 administration in *db/db* mice and lean mice. ZLN005 (15 mg · kg^{-1} · day^{-1}) was administered orally for 6 weeks, and metformin (250 mg · kg^{-1} · day^{-1}) was used as a positive control. During the treatment, ZLN005 did not affect body weight gain or food intake in either *db/db* mice or lean mice (Fig. 5*A* and *B*). In lean mice, plasma glucose generally was unchanged by ZLN005 treatment. In *db/db* mice, however, random blood glucose and fasting blood glucose levels decreased significantly over 4 weeks by ZLN005 and metformin treatment (Fig. 5*C* and *D*). ZLN005 did not alter glucose tolerance in lean mice, but in *db/db* mice it improved glucose clearance, as evidenced by the approximately 14% decrease in the area under the curve (AUC) (Fig. 5*E*). An insulin tolerance test revealed that treatment with ZLN005 significantly decreased insulin resistance in *db/db* mice, as evidenced by the approximately 18% decrease in the AUC (Fig. 5*F*). A PTT also was performed in *db/db* mice, and ZLN005 improved pyruvate tolerance, as evidenced by the 16% decrease in the AUC (Fig. 5*G*).

In *db/db* mice, plasma NEFA and triglyceride levels were decreased by 20% and 37%, respectively, and cholesterol was decreased by 10% (Table 1) with ZLN005 treatment. Plasma insulin and β-hydroxybutyrate content, liver/body-weight index and adipose composition, and muscle and liver triglyceride levels, however, were not ameliorated by treatment with ZLN005 or metformin.

Together, these results indicated that ZLN005 had antihyperglycemia and antihyperlipidemia effects and increased insulin sensitivity in *db/db* mice but not lean mice. These results suggested that ZLN005 might act selectively in the diabetic mouse model and have no adverse effects on normal lean mice.

Tissue-specific efficacy of ZLN005 in skeletal muscle and liver tissue of diabetic *db/db* mice. To clarify the tissue-specific efficacy, we found that chronic treatment with ZLN005 led to significant induction of *PGC-1α* mRNA expression and PGC-1α target genes in the gastrocnemius, including *GLUT4* and mitochondria OXPHOS genes such as *ERRα*, cytochrome-c, *cox5b*, *ATPase-F1α*, and uncoupling protein 3. Genes related to FAO, such as medium-chain acyl-CoA dehydrogenase (*MCAD*) and long-chain acyl-CoA dehydrogenase, also were induced. However, *NRF1* and carnitine palmitoyl transferase 1 remained unchanged (Fig. 6*A*).

We also investigated gene expression in liver tissue. Unlike in skeletal muscle, *PGC-1α* mRNA was downregulated by 34% compared with the vehicle group. Its downstream gluconeogenic genes, including glucose-6-phosphatase (*G6Pase*) and *PEPCK*, were reduced by 31% and 27%, respectively (Fig. 6*B*), in response to ZLN005 treatment. PGC-1α is known to coordinate the mitochondria OXPHOS and FAO in liver, so the expression of mitochondria OXPHOS genes, such as cytochrome-c, *ERRα*, *cox5b*, and *ATPase-F1α*, also were investigated. However, no reduction was observed in the mRNA level of these genes. Similarly, no changes in carnitine palmitoyl transferase 1, *MCAD*, and acyl-CoA oxidase were observed.

PGC-1α has emerged as a master regulator of mitochondria, and mitochondrial biogenesis resulting from an increased number of mitochondrial DNA copies. Indeed, mitochondrial DNA was increased (31%) by ZLN005 in the gastrocnemius of *db/db* mice, an effect that was not observed in liver (Fig. 6*C*). We also measured AMPK and ACC phosphorylation in abdominal muscle and liver tissue of *db/db* mice. Consistent with the results found at the cellular level, AMPK and ACC phosphorylation were increased in abdominal muscle but not in liver tissue (Fig. 6*D* and *E*). These differing effects suggested that ZLN005 increased *PGC-1α* expression in a tissue-specific manner in vivo.

DISCUSSION

Transcription cofactor PGC-1α is precisely regulated in a number of metabolic tissues and physiological contexts, such as in response to fasting in the liver and exercise in muscle. It is dysregulated in pathological states, such as mitochondrial dysfunction in skeletal muscle and hypergluconeogenesis. It may, therefore, be a potential target for drug discovery in the treatment of metabolic syndromes. Arany et al. (34) recently set up an HTS method for the identification of small molecules that induced *PGC-1α* in primary skeletal muscle cells, demonstrating that PGC-1α could be regulated. Here, we used a luciferase assay to identify small molecules and demonstrate positive effects on *PGC-1α* transcriptional regulation. During this process the shortcomings of a luciferase assay were uncovered: small molecules inhibiting luciferase activity affected the outcome of the HTS.

Exercise induces *PGC-1α* in skeletal muscle, where it induces *GLUT4* and mitochondrial OXPHOS. Increasing PGC-1α activity in skeletal muscle should, therefore, be

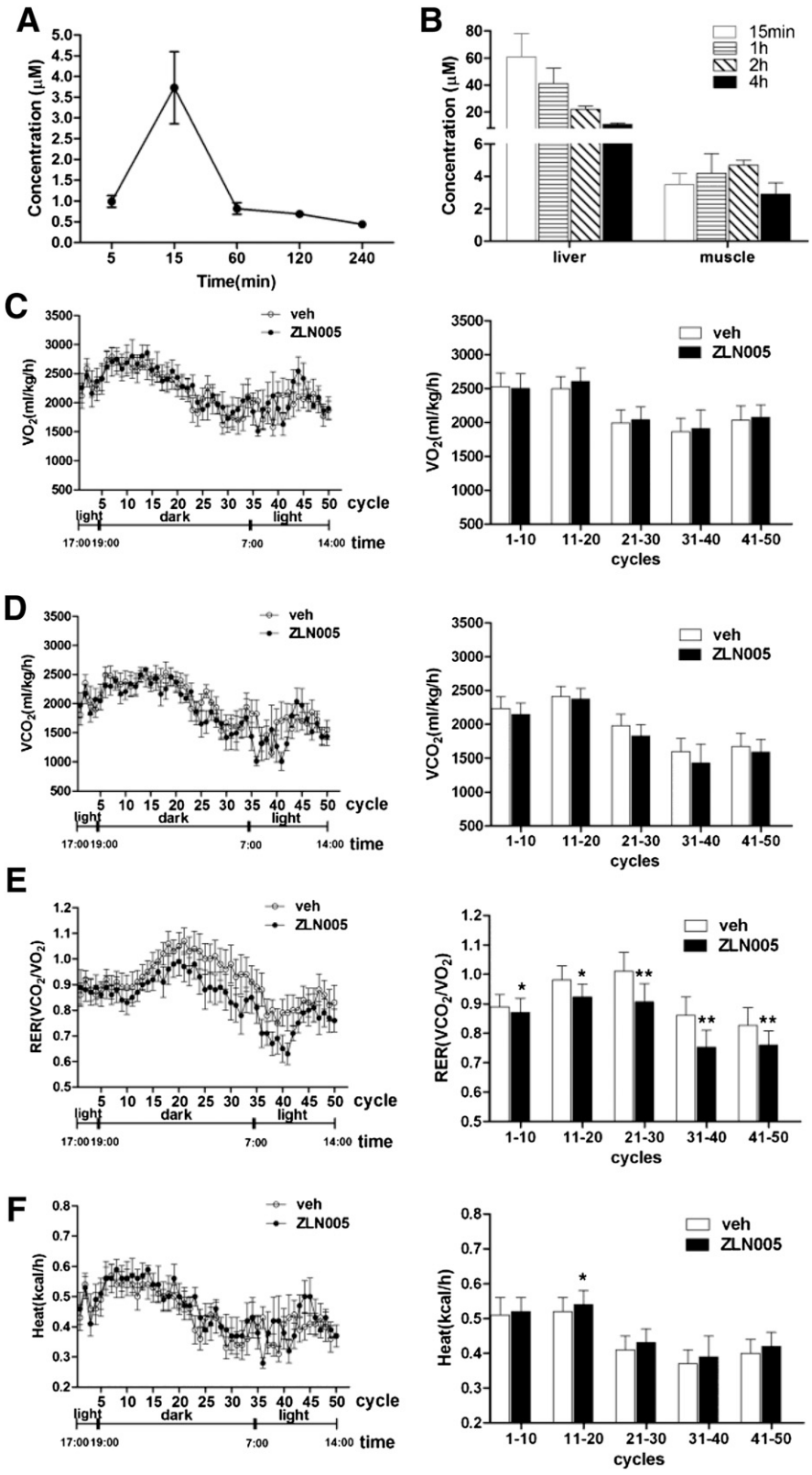

FIG. 4. Chronic effects of ZLN005 on RER in *db/db* mice. *A*: Mean plasma concentration time profiles of ZLN005 after a single oral dose (15 mg · kg^{-1}) in *db/db* mice (n = 3). *B*: Distribution of ZLN005 in tissues harvested after a single oral dose (n = 3). *C* and *D*: For RER measurement, 8-week-old *db/db* mice were gavaged with vehicle (0.5% methylcellulose) or ZLN005 (15 mg · kg^{-1} · day^{-1}) for 2 weeks. After a 4-h rest, mice were placed in a metabolic chamber and observed over a 21-h period (n = 6–8). Energy expenditure was evaluated by oxygen consumption (V_{O_2}) and carbon dioxide release (V_{CO_2}). *E* and *F*: Changes in RER and heat throughout the monitoring period (white circle = vehicle, black circle = ZLN005). The adjacent bar graphs represent the average for each group. *$P < 0.05$, **$P < 0.01$ compared with vehicle.

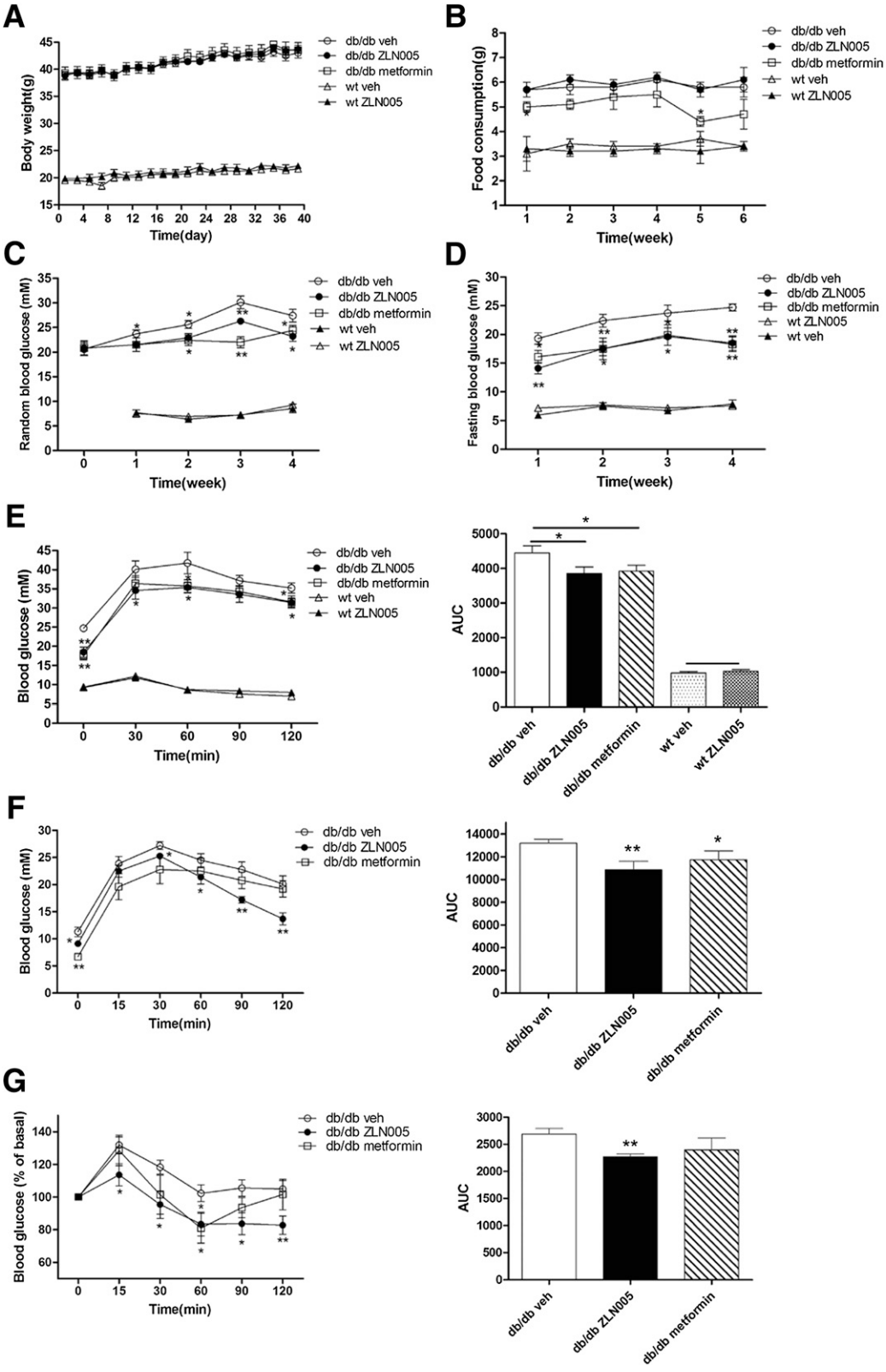

FIG. 5. Antidiabetic effects of ZLN005 in *db/db* mice. Eight-week-old *db/db* mice were gavaged with vehicle (0.5% methylcellulose), ZLN005 (15 mg · kg^{-1} · day^{-1}), or metformin (250 mg · kg^{-1} · day^{-1}) (n = 6–8) and lean mice (wt) were gavaged with vehicle (0.5% methylcellulose) and ZLN005 (15 mg · kg^{-1} · day^{-1}). *A*: Body weight. *B*: Food consumption. *C*: Random blood glucose. *D*: Fasting blood glucose. *E*: Blood glucose levels after an intraperitoneal glucose load (1.5 g · kg^{-1}) performed after 4 weeks of treatment. The areas under the curve are indicators of glucose clearance. *F*: Blood glucose levels after an intraperitoneal insulin load (1 unit insulin · kg^{-1}) performed after 5 weeks of treatment in *db/db* mice. The areas under the curve are indicator of insulin clearance. *G*: Blood glucose levels after an intraperitoneal sodium pyruvate load (1.5 g · kg^{-1}) given after 5 weeks of treatment in *db/db* mice. The areas under the curve are indicators of pyruvate clearance (white circle = *db/db* vehicle, black circle = *db/db* ZLN005, white square = *db/db* metformin, white triangle = wt vehicle, black triangle = wt ZLN005). *P < 0.05, **P < 0.01 compared with vehicle.

TABLE 1
Chronic effects of ZLN005 and metformin on metabolic variables in *db/db* mice

Variable	Treatment		
	Vehicle	ZLN005	Metformin
Plasma triglyceride (mmol)	0.52 ± 0.07	0.33 ± 0.02**	0.36 ± 0.03*
Plasma NEFA (mEq/L)	1.02 ± 0.07	0.82 ± 0.07*	0.85 ± 0.04*
Plasma cholesterol (mmol)	2.38 ± 0.02	2.14 ± 0.09*	2.21 ± 0.07
Plasma insulin (ng/mL)	1.41 ± 0.18	2.26 ± 0.73	2.33 ± 0.59
Plasma β-hydroxybutyrate (mmol)	0.65 ± 0.09	0.64 ± 0.06	0.62 ± 0.12
Liver (% body weight)	4.83 ± 0.16	4.82 ± 0.14	5.24 ± 0.04*
Epididymal fat (% body weight)	4.96 ± 0.18	4.76 ± 0.15	4.93 ± 0.03
Perirenal fat (% body weight)	2.57 ± 0.09	2.62 ± 0.08	2.44 ± 0.07
Subcutaneous fat (% body weight)	6.36 ± 0.37	6.09 ± 0.33	7.44 ± 0.41*
Hepatic triglyceride (μmol/g)	161.3 ± 14.7	135.3 ± 11.2	206.2 ± 20.0*
Muscle triglyceride (μmol/g)	130.4 ± 7.5	126.4 ± 19.0	122.1 ± 13.5

The data represent the mean ± SE of 6–8 mice. *$P < 0.05$; **$P < 0.01$ compared with the vehicle group.

beneficial in metabolic disorders. First, we chose L6 myotubes to validate ZLN005. We found that it increased *PGC-1α* and downstream gene expression. Consistent with increased gene expression, FAO and glucose uptake also were up-regulated in L6 myotubes. An siRNA study then demonstrated that ZLN005-stimulated oxidation of palmitic acid was dependent on PGC-1α.

In the chronic treatment of *db/db* mice, the GLUT4 and mitochondrial OXPHOS genes were up-regulated in the gastrocnemius. Some of the regulators of FAO, such as long-chain acyl-CoA dehydrogenase and *MCAD*, also were up-regulated by ZLN005, consistent with ZLN005 promoting palmitic acid oxidation in L6 myotubes. The number of mitochondria was increased simultaneously, demonstrating that ZLN005 might promote mitochondria biogenesis.

Liver gluconeogenesis is known to be highly regulated by PGC-1α (19). Excessive gluconeogenesis is one of the symptoms of T2DM. We observed down-regulation of hepatic expression of *PGC-1α*, *PEPCK*, and *G6Pase* and improvement of PTT results in *db/db* mice. Several studies have shown that liver-specific down-regulation of *PGC-1α* leads to defects in lipid metabolism and hepatic insulin resistance (41), suggesting PGC-1α regulation must be tightly connected to lipid homeostasis and glucose metabolism.

Because decreased expression of *PGC-1α* was observed in liver tissue, the influence of PGC-1α on FAO and mitochondria biogenesis genes was explored next. It is noteworthy that these expression levels remained unchanged. It has been reported that mice with a germ line—targeted disruption of *PGC-1α* exhibited normal mitochondrial abundance and morphology in the liver (42). Thus, compensatory pathways to maintain the function of liver mitochondria might exist. It also was reported that increased insulin sensitivity might elicit the phosphorylation and inhibition of PGC-1α through kinase Akt2/protein kinase B-β (43). In contrast to the effects observed in *db/db* mice, ZLN005 had no effect on the expression of *PGC-1α* and *PEPCK* in primary hepatocytes. Therefore, we speculated that alterations in *PGC-1α* in the liver tissue of *db/db* mice might be a secondary phenomenon.

The effect of ZLN005 incorporation in vivo in lean mice and *db/db* mice was tested. After a 2-week treatment, a reduction in the RER was observed, which reflected the preferential use of lipids over carbohydrates as a source of energy. After a 6-week treatment, ZLN005 improved glucose homeostasis and insulin sensitivity, possibly from muscle glucose uptake because an increase in *GLUT4* expression was observed. This effect also was possible through diminished production of hepatic glucose, a principal constituent of whole-body glucose homeostasis. The improvement in PTT values may have resulted from down-regulation of *PEPCK* and *G6Pase* gene expression. Lipid profiles, such as triglycerides, NEFAs, and cholesterol levels, were reduced, potentially as a consequence of enhanced use of whole-body fat.

Because PGC-1α is activated in pancreatic β-cells in animal models of obesity and T2DM, poor transcriptional regulation might lead to a deficiency in insulin secretion (44). The unchanged plasma insulin levels suggested that ZLN005 might not show adverse effects on pancreatic β-cells. In addition, the antidiabetic action of ZLN005 was not a direct consequence of food intake because body weight gain and food intake differences between groups were minimal. Furthermore, ZLN005 had no major side effects in lean mice, indicating that it worked specifically in diabetic mice. For preliminary safety evaluation, Sprague-Dawley rats were administered either vehicle or ZLN005 (75 $mg \cdot kg^{-1} \cdot day^{-1}$) orally for 14 days. All the animals survived, and no obvious change in the body weight gain or metabolic parameters was observed (Supplementary Tables 2–4).

At the *PGC-1α* promoter, there is a MEF binding site for the transcription factor MEF2, an insulin receptor substrate binding site for forkhead box class-O and a CRE binding site for activating transcription factor 2 and CREBP, all of which enhance PGC-1α transcription (32). In this case, we investigated the effect of ZLN005 on CRE and MEF binding sites and found that MEF was necessary for the up-regulation of *PGC-1α* in L6 myocytes.

A number of intracellular pathways are known to impinge on PGC-1α, including signaling by cAMP, AMPK, Ca^{2+}, and p38 MAPK (40,45,46). To investigate the mechanism by which ZLN005 enhanced *PGC-1α* expression in L6 myotubes, we sought to identify signaling pathways and found that phosphorylation of Thr-180/Tyr-182 in p38 MAPK, which phosphorylates and activates MEF2 and activating transcription factor 2, was not increased after treatment with ZLN005. In addition, phosphorylation of Ser-133 of CREBP, which can be stimulated by Ca^{2+} signaling through calmodulin-dependent protein kinase IV

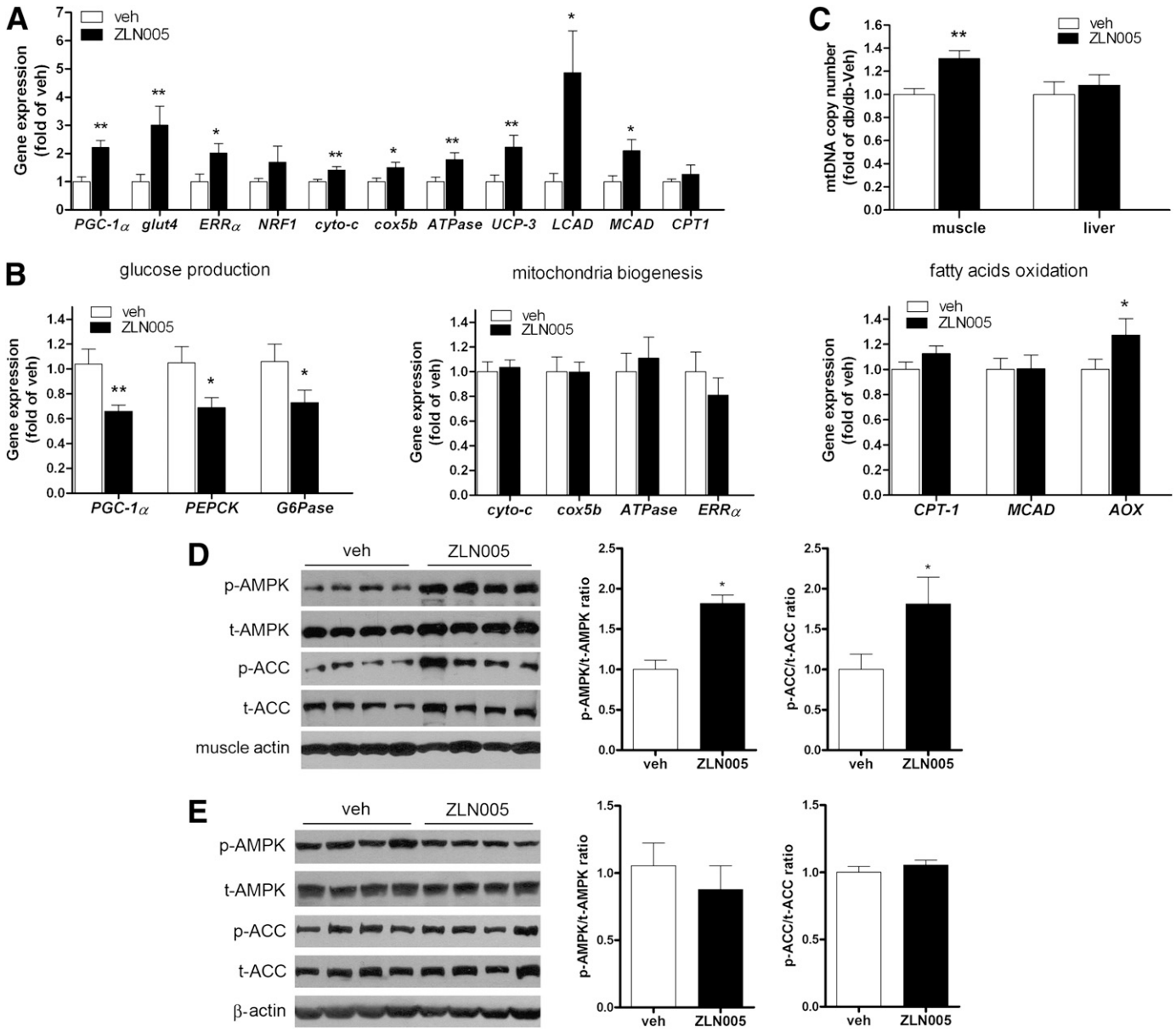

FIG. 6. Chronic effects of ZLN005 in skeletal muscle and liver of *db/db* mice. *A*: RT-PCR analysis was used to measure mRNA levels from the gastrocnemius of animals (n = 6–8). *B*: RT-PCR analysis was used to measure the mRNA levels of the glucose production gene, mitochondrial biogenesis gene, and fatty acid oxidation gene in livers of animals (n = 6–8). *C*: Mitochondrial DNA copy number of gastrocnemius muscle and liver from ZLN005-treated and untreated *db/db* mice (n = 6–8). *D* and *E*: AMPK and ACC phosphorylation from the abdominal muscle (*D*) and liver (*E*) of *db/db* mice. The ratio of the phosphorylation level to the protein level of AMPK and ACC was determined. *$P < 0.05$, **$P < 0.01$ compared with vehicle.

and calcineurin A, also did not change (32). However, AMPK was activated by ZLN005 in L6 myotubes and the muscle tissue of *db/db* mice, and *PGC-1α* expression and glucose uptake are dependent on AMPK activation at the cellular level. To further address this issue, we found ZLN005 activated AMPK by mildly uncoupling mitochondria to increase the cellular ADP-to-ATP ratio. The weak uncoupling of mitochondria leading to a beneficial effect on metabolism was reported previously (47). AMPK is an energy sensor that is activated upon depletion of energy (48) and phosphorylates PGC-1α on Thr-177 and Ser-538 in skeletal muscle (49). It is plausible that AMPK phosphorylated PGC-1α and that PGC-1α then acted through positive feedback, binding with MEF2C to increase its own gene expression in myotubes (27). It is interesting that the AMPK pathway did not seem to be affected in rat primary hepatocytes (Supplementary Fig. 2) or the liver tissue of *db/db* mice, possibly because of the different energy states of the two types of cells. Considering the discrepancy in L6 myotubes and primary hepatocytes, and because MEF2 proteins are expressed predominantly in muscle and the brain (50), we speculated that ZLN005 regulates *PGC-1α* through muscle cell–specific transcription factors such as MEF2. Thus, the down-regulation of *PGC-1α* mRNA in the liver tissue of *db/db* mice might occur as a result.

Overall, our results demonstrated that small molecule–mediated tissue-specific activation of *PGC-1α* in skeletal muscle is feasible and that the novel compound ZLN005 exerts beneficial effects in an animal model of T2DM. These results further support the potential of PGC-1α as a drug target for the treatment of T2DM and metabolic syndromes.

ACKNOWLEDGMENTS

This work was supported by the National Natural Science Foundation of China (Grants 81001463 and 81125023), the National Science and Technology Major Projects for Major New Drugs Innovation and Development (Grant 2012ZX09304011), the National Program on Key Basic Research Project (Grants 2012CB524906 and G1998051104), and the Shanghai Commission of Science and Technology (Grant 11DZ2292200).

No potential conflicts of interest relevant to this article were reported.

L.-N.Z. contributed to research data, discussion, and preparation of the manuscript. F.W., C.-M.X., and T.-C.D. contributed to the animal experiments. H.-Y.Z. contributed to the synthesis of compounds. Y.-Y.F., Y.-Y.L., M.G., and L.-Y.W. contributed to the discussion and research data. J.-Y.L., J.-K.S., and J.L. contributed to the study design, discussion, and editing of the manuscript. J.Y.-L. is the guarantor of this work and, as such, had full access to all the data in the study and takes responsibility for the integrity of the data and the accuracy of data analysis.

REFERENCES

1. St-Pierre J, Lin J, Krauss S, et al. Bioenergetic analysis of peroxisome proliferator-activated receptor gamma coactivators 1alpha and 1beta (PGC-1alpha and PGC-1beta) in muscle cells. J Biol Chem 2003;278:26597–26603
2. Scarpulla RC. Metabolic control of mitochondrial biogenesis through the PGC-1 family regulatory network. Biochim Biophys Acta 2011;1813:1269–1278
3. Lin JD. Minireview: the PGC-1 coactivator networks: chromatin-remodeling and mitochondrial energy metabolism. Mol Endocrinol 2009;23:2–10
4. Handschin C, Spiegelman BM. The role of exercise and PGC1alpha in inflammation and chronic disease. Nature 2008;454:463–469
5. Puigserver P, Adelmant G, Wu Z, et al. Activation of PPARgamma coactivator-1 through transcription factor docking. Science 1999;286:1368–1371
6. Esterbauer H, Oberkofler H, Krempler F, Patsch W. Human peroxisome proliferator activated receptor gamma coactivator 1 (PPARGC1) gene: cDNA sequence, genomic organization, chromosomal localization, and tissue expression. Genomics 1999;62:98–102
7. Knutti D, Kaul A, Kralli A. A tissue-specific coactivator of steroid receptors, identified in a functional genetic screen. Mol Cell Biol 2000;20:2411–2422
8. Asher G, Schibler U. Crosstalk between components of circadian and metabolic cycles in mammals. Cell Metab 2011;13:125–137
9. Handschin C, Spiegelman BM. Peroxisome proliferator-activated receptor gamma coactivator 1 coactivators, energy homeostasis, and metabolism. Endocr Rev 2006;27:728–735
10. Liang H, Ward WF. PGC-1alpha: a key regulator of energy metabolism. Adv Physiol Educ 2006;30:145–151
11. Jeninga EH, Schoonjans K, Auwerx J. Reversible acetylation of PGC-1: connecting energy sensors and effectors to guarantee metabolic flexibility. Oncogene 2010;29:4617–4624
12. Finck BN, Kelly DP. PGC-1 coactivators: inducible regulators of energy metabolism in health and disease. J Clin Invest 2006;116:615–622
13. Vimaleswaran KS, Radha V, Ghosh S, et al. Peroxisome proliferator-activated receptor-gamma co-activator-1alpha (PGC-1alpha) gene polymorphisms and their relationship to Type 2 diabetes in Asian Indians. Diabet Med 2005;22:1516–1521
14. Muller YL, Bogardus C, Pedersen O, Baier L. A Gly482Ser missense mutation in the peroxisome proliferator-activated receptor gamma coactivator-1 is associated with altered lipid oxidation and early insulin secretion in Pima Indians. Diabetes 2003;52:895–898
15. Oberkofler H, Linnemayr V, Weitgasser R, et al. Complex haplotypes of the PGC-1alpha gene are associated with carbohydrate metabolism and type 2 diabetes. Diabetes 2004;53:1385–1393
16. Andrulionytè L, Zacharova J, Chiasson JL, Laakso M; STOP-NIDDM Study Group. Common polymorphisms of the PPAR-gamma2 (Pro12Ala) and PGC-1alpha (Gly482Ser) genes are associated with the conversion from impaired glucose tolerance to type 2 diabetes in the STOP-NIDDM trial. Diabetologia 2004;47:2176–2184
17. Hara K, Tobe K, Okada T, et al. A genetic variation in the PGC-1 gene could confer insulin resistance and susceptibility to Type II diabetes. Diabetologia 2002;45:740–743
18. Kim JH, Shin HD, Park BL, et al. Peroxisome proliferator-activated receptor gamma coactivator 1 alpha promoter polymorphisms are associated with early-onset type 2 diabetes mellitus in the Korean population. Diabetologia 2005;48:1323–1330
19. Yoon JC, Puigserver P, Chen G, et al. Control of hepatic gluconeogenesis through the transcriptional coactivator PGC-1. Nature 2001;413:131–138
20. Koo SH, Satoh H, Herzig S, et al. PGC-1 promotes insulin resistance in liver through PPAR-alpha-dependent induction of TRB-3. Nat Med 2004;10:530–534
21. Attie AD, Kendziorski CM. PGC-1alpha at the crossroads of type 2 diabetes. Nat Genet 2003;34:244–245
22. Mootha VK, Lindgren CM, Eriksson KF, et al. PGC-1alpha-responsive genes involved in oxidative phosphorylation are coordinately downregulated in human diabetes. Nat Genet 2003;34:267–273
23. Patti ME, Butte AJ, Crunkhorn S, et al. Coordinated reduction of genes of oxidative metabolism in humans with insulin resistance and diabetes: Potential role of PGC1 and NRF1. Proc Natl Acad Sci U S A 2003;100:8466–8471
24. Michael LF, Wu Z, Cheatham RB, et al. Restoration of insulin-sensitive glucose transporter (GLUT4) gene expression in muscle cells by the transcriptional coactivator PGC-1. Proc Natl Acad Sci U S A 2001;98:3820–3825
25. Wenz T, Rossi SG, Rotundo RL, Spiegelman BM, Moraes CT. Increased muscle PGC-1alpha expression protects from sarcopenia and metabolic disease during aging. Proc Natl Acad Sci U S A 2009;106:20405–20410
26. Qiu BY, Turner N, Li YY, et al. High-throughput assay for modulators of mitochondrial membrane potential identifies a novel compound with beneficial effects on db/db mice. Diabetes 2010;59:256–265
27. Handschin C, Rhee J, Lin J, Tarr PT, Spiegelman BM. An autoregulatory loop controls peroxisome proliferator-activated receptor gamma coactivator 1alpha expression in muscle. Proc Natl Acad Sci U S A 2003;100:7111–7116
28. Lagouge M, Argmann C, Gerhart-Hines Z, et al. Resveratrol improves mitochondrial function and protects against metabolic disease by activating SIRT1 and PGC-1alpha. Cell 2006;127:1109–1122
29. Frezza C, Cipolat S, Scorrano L. Organelle isolation: functional mitochondria from mouse liver, muscle and cultured fibroblasts. Nat Protoc 2007;2:287–295
30. Turner N, Li JY, Gosby A, et al. Berberine and its more biologically available derivative, dihydroberberine, inhibit mitochondrial respiratory complex I: a mechanism for the action of berberine to activate AMP-activated protein kinase and improve insulin action. Diabetes 2008;57:1414–1418
31. Vichai V, Kirtikara K. Sulforhodamine B colorimetric assay for cytotoxicity screening. Nat Protoc 2006;1:1112–1116
32. Fernandez-Marcos PJ, Auwerx J. Regulation of PGC-1α, a nodal regulator of mitochondrial biogenesis. Am J Clin Nutr 2011;93:884S–890S
33. Arany Z. PGC-1 coactivators and skeletal muscle adaptations in health and disease. Curr Opin Genet Dev 2008;18:426–434
34. Arany Z, Wagner BK, Ma Y, Chinsomboon J, Laznik D, Spiegelman BM. Gene expression-based screening identifies microtubule inhibitors as inducers of PGC-1alpha and oxidative phosphorylation. Proc Natl Acad Sci U S A 2008;105:4721–4726
35. Vega RB, Huss JM, Kelly DP. The coactivator PGC-1 cooperates with peroxisome proliferator-activated receptor alpha in transcriptional control of nuclear genes encoding mitochondrial fatty acid oxidation enzymes. Mol Cell Biol 2000;20:1868–1876
36. Liu C, Lin JD. PGC-1 coactivators in the control of energy metabolism. Acta Biochim Biophys Sin (Shanghai) 2011;43:248–257
37. Zong H, Ren JM, Young LH, et al. AMP kinase is required for mitochondrial biogenesis in skeletal muscle in response to chronic energy deprivation. Proc Natl Acad Sci U S A 2002;99:15983–15987
38. Akimoto T, Pohnert SC, Li P, et al. Exercise stimulates Pgc-1alpha transcription in skeletal muscle through activation of the p38 MAPK pathway. J Biol Chem 2005;280:19587–19593
39. Zhao M, New L, Kravchenko VV, et al. Regulation of the MEF2 family of transcription factors by p38. Mol Cell Biol 1999;19:21–30
40. Puigserver P, Rhee J, Lin J, et al. Cytokine stimulation of energy expenditure through p38 MAP kinase activation of PPARgamma coactivator-1. Mol Cell 2001;8:971–982
41. Estall JL, Kahn M, Cooper MP, et al. Sensitivity of lipid metabolism and insulin signaling to genetic alterations in hepatic peroxisome proliferator-activated receptor-gamma coactivator-1alpha expression. Diabetes 2009;58:1499–1508
42. Lin J, Wu PH, Tarr PT, et al. Defects in adaptive energy metabolism with CNS-linked hyperactivity in PGC-1alpha null mice. Cell 2004;119:121–135

43. Li X, Monks B, Ge Q, Birnbaum MJ. Akt/PKB regulates hepatic metabolism by directly inhibiting PGC-1alpha transcription coactivator. Nature 2007; 447:1012–1016
44. Yoon JC, Xu G, Deeney JT, et al. Suppression of beta cell energy metabolism and insulin release by PGC-1alpha. Dev Cell 2003;5:73–83
45. Barger PM, Browning AC, Garner AN, Kelly DP. p38 mitogen-activated protein kinase activates peroxisome proliferator-activated receptor alpha: a potential role in the cardiac metabolic stress response. J Biol Chem 2001; 276:44495–44501
46. Knutti D, Kressler D, Kralli A. Regulation of the transcriptional coactivator PGC-1 via MAPK-sensitive interaction with a repressor. Proc Natl Acad Sci U S A 2001;98:9713–9718
47. Martineau LC. Large enhancement of skeletal muscle cell glucose uptake and suppression of hepatocyte glucose-6-phosphatase activity by weak uncouplers of oxidative phosphorylation. Biochim Biophys Acta 2012; 1820:133–150
48. Steinberg GR, Kemp BE. AMPK in Health and Disease. Physiol Rev 2009; 89:1025–1078
49. Jäger S, Handschin C, St-Pierre J, Spiegelman BM. AMP-activated protein kinase (AMPK) action in skeletal muscle via direct phosphorylation of PGC-1alpha. Proc Natl Acad Sci U S A 2007;104:12017–12022
50. Potthoff MJ, Olson EN. MEF2: a central regulator of diverse developmental programs. Development 2007;134:4131–4140